Bidirectional reflectance scale comparison between NIST and PTB

Catherine C. Cooksey,[1] Maria E. Nadal,[1] David W. Allen,[1] Kai-Olaf Hauer,[2] and Andreas Höpe[2]

[1]*National Institute of Standards and Technology, 100 Bureau Drive, Gaithersburg, MD 20899-8442*
[2]*Physikalisch-Technische Bundesanstalt (PTB), Bundesallee 100, 38116 Braunschweig, Germany*

**Corresponding authors: catherine.cooksey@nist.gov, andreas.hoepe@ptb.de*

Received Month X, XXXX; revised Month X, XXXX; accepted Month X, XXXX; posted Month X, XXXX (Doc. ID XXXXX); published Month X, XXXX

Interlaboratory comparisons, referred to as key comparisons, are completed for many metrological units within the framework of the Mutual Recognition Arrangement (MRA) of the BIPM (Bureau International des Poids et Mesures). These comparisons are the responsibility of Consultative Committees (CC) of the different metrological areas. In the case of the CCPR (Consultative Committee for Photometry and Radiometry), there are currently about 20 key comparisons for various measurands. While interest in the field of bidirectional reflectance has been growing in recent years among users in industry and research and development, there is currently no dedicated key comparison to demonstrate scale conformity. This is the basis of the comparison of the bidirectional reflectance scales between the National Institute of Standards and Technology (NIST) and the Physikalisch-Technische Bundesanstalt (PTB). Measurements of two distinct sets of white diffuse reflectance standards, two sintered polytetrafluoroethylene (PTFE) samples and two matte ceramic samples were performed using the common and widely-used 0:45 geometry. The wavelength range of the comparison spans the ultraviolet ($\lambda \geq 330$ nm) to the near infrared ($\lambda \leq 1150$ nm), a technically important region. In total 5 different facilities participated in this bilateral investigation. The results of the comparison show good agreement within the combined uncertainties.

OCIS codes: (120.1840) Densitometers, reflectometers; (120.5700) Reflection; (290.1483) BSDF, BRDF, and BTDF
http://dx.doi/org/10.1364/AO.99.099999

1. Introduction

Requests for measurements and calibrations using bidirectional diffuse reflection geometries have substantially increased in recent years. The driving forces behind this trend are the stringent requirements from industry and research and development (R&D). The industrial demands are due in large part to a variety of new materials, so-called gonioapparent or goniocromatic materials, whose visual appearance changes significantly depending on the angular pair of irradiation and viewing [1–3]. Such materials include metallic paint finishes, lustre pigments and interferometric coatings [4–6]. The R&D demands arise from sophisticated applications, such as material characterizations of space-based implementations (i.e., specific satellite components) [7] or the radiometric in-orbit traceability of earth-observation satellites via calibrated reflectance standards [8,9]. For both cases, the growing need for bidirectional reflectance measurements using geometries with arbitrary angles of incidence and reflection located within the half-space above the sample under test has resulted in the development of elaborate, custom-built gonioreflectometers [10–16].

In particular, the visual appearance of industrial products, which is a bidirectional characteristic, is becoming more and more relevant as customers place increasing importance on the aesthetic appeal of merchandise. This has led to the development of commercially available, multi-angle spectrophotometers that enable reflectance measurements of the sample under test using up to 14 different angular combinations. Many of these geometries are recommended in standards of the Deutsches Institut für Normung e.V. (DIN) and ASTM International [17,18]. Typically, these commercial multi-angle instruments are relative measuring devices requiring traceability to the absolute reflectance scale maintained at dedicated NMIs (National Metrology Institutes) via calibrated diffuse reflection standards in the desired bidirectional reflection geometry.

Currently, bidirectional reflectance scales are not included in the key comparisons arranged by the Consultative Committee of Photometry and Radiometry (CCPR) of the Bureau International des Poids et Mesures (BIPM). International comparisons on diffuse reflectance have focused on directional-hemispherical or hemispherical-directional reflectance, which are based on integrating sphere measurements. The most recently completed key comparison, CCPR-K5: Spectral diffuse reflectance, had participants from 13 different countries worldwide, including NIST and PTB [19].

Key comparisons are a critical component of the Comité International des Poids et Mesures (CIPM) Mutual Recognition Arrangement (MRA) [20]. They establish the degree of equivalence of national measurement scales and substantiate the published Calibration and Measurement Capabilities (CMCs) of an NMI found in Appendix C of the CIPM MRA, thereby supporting trade and commerce in the global marketplace. Thus, in the absence of a key comparison on bidirectional reflectance, NIST and PTB arranged a bilateral comparison of their respective scales for the 0:45 geometry. (In-plane, bidirectional geometries are designated as θ_i:θ_r, where θ_i is the angle of incident radiation with respect to the surface normal and θ_r is the detection angle of reflection [21].) This geometrical configuration was selected based on its widespread use. Like the 45:0 geometry, it is recommended by the CIE (Commission Internationale de l´Eclairage, International Commission on Illumination) [22].

Here, we present results of this bilateral comparison, which spanned the spectral region from $\lambda = 330$ nm in the ultraviolet (UV) through the visible (Vis) to $\lambda = 1150$ nm in the near infrared (NIR). Four reflectance standards were exchanged between NIST and PTB: two sintered polytetrafluoroethylene (PTFE) samples and two matte ceramic samples. The two types of standards were selected based on their different material composition and distinct spectral properties. Sintered PTFE is strongly reflecting and spectrally flat over the investigated wavelength range; whereas the reflectance of the ceramic exhibits a steep decrease for wavelengths below 450 nm. Despite varying measurement approaches (absolute versus relative measurements and different methods of spectral discrimination), the resulting degrees of equivalence demonstrate excellent agreement of the 0:45 reflectance scales of NIST and PTB.

2. Measurements

A. Measurement Protocol

This comparison involved the exchange of four reflectance standards, two sintered PTFE samples and two matte ceramic samples. The sintered PTFE standards were 5 cm by 5 cm square, and were identified as PTFE #1 and PTFE #2. The two matte ceramic standards were 88% white and also 5 cm by 5 cm square. These standards were identified as Ceramic #45 and Ceramic #46.

NIST and PTB measured the 0:45 reflectance factor for each of the four comparison items at 5 nm increments within the silicon detection range (330 nm to 1150 nm), and calculated the combined expanded uncertainties ($k = 2$).

The following sub-sections provide descriptions of each instrument and measurement methods employed. Additional details of specific wavelength ranges and other measurement parameters can be found in Table 1.

B. PTB Measurements

PTB operates a robot-based gonioreflectometer for the calibration of diffuse reflectance standards for bidirectional geometries [10,11,23]. The system is capable of performing measurements within the entire hemisphere above the sample under test, and the orientation of the angles of incidence and detection, with respect to each other, can be chosen arbitrarily.

The gonioreflectometer acquires absolute measurements of reflectance and uses broadband irradiation of the sample with spectrally selected detection of the reflected radiation. A schematic of the instrument is shown in Figure 1. Briefly, unfiltered and unpolarized irradiation is generated by a sphere radiator, which consists of a small integrating sphere with an internal diameter of 150 mm and a built-in quartz tungsten halogen (QTH) lamp. This light source provides a near-Lambertian beam profile, with the spatial variation of the emitted radiance on the order of ± 0.2 % [24]. The sphere radiator is mounted on a large rotation stage that can be rotated 360° around the sample to establish the angle of incidence. The sample is mounted on a small five-axis industrial robot, which can orient the sample for both in-plane (sample normal lies within the plane of reflection) and out-of-plane (sample normal lies outside of the plane of reflection) measurements. The position of the detection system is fixed and consists of a set of five folding- and focussing-mirrors, a monochromator, and the detector.

The spectral reflectance factor $R(\lambda)$ is calculated based on the following equation:

$$R(\lambda) = \frac{\pi \cdot {r_S}^2}{A_S \cdot \cos\theta_i} \cdot \frac{S_r'(\lambda)}{S_i'(\lambda)} \qquad (1)$$

where r_s is the distance between the sample and the aperture of the sphere radiator, A_s is the area of this aperture, and θ_i is the incident angle of the radiation, or more specifically, the angle between the vector of the surface normal of the sample and the direction vector of the directional incident radiation. $S_r'(\lambda)$ is the net signal due to the reflected radiation and $S_i'(\lambda)$ is the net signal due to the incident radiation, such that both signals are corrected for the dark current.

For each wavelength, the signals are measured in the following sequence: reflected signal, dark signal in the reflected position, incident signal, dark signal in the incident position. The dark signals are obtained by closing a shutter in the projection beam path of the detection. The comparison items were aligned to the robotic hand of the gonioreflectometer with

the dorsal orientation mark upright due to a dedicated adjustment procedure to assure that the surface is collinear with the combined rotation axis of the large rotation stage and the base axis of the robot.

C. NIST Measurements

At NIST, there are two reflectance facilities. The first is the NIST Spectral Tri-function Automated Reference Reflectometer (STARR), which serves as the national reference instrument for spectral reflectance measurements. The instrument was designed to calibrate spectrally neutral, non-fluorescent specular and diffuse samples for both directional-hemispherical and bidirectional reflectance measurement geometries. The second reflectance facility is the NIST Goniospectrometer. The primary purpose of this multi-functional facility is to measure the spectral reflectance of colored samples over a wide range of illumination and viewing angles, including out-of-plane geometries. This capability is important for the colorimetric characterization of complex surfaces, such as gonioapparent or retroreflective coatings and to disseminate color standards to the color and appearance community.

1 NIST STARR

STARR acquires absolute measurements of bidirectional reflectance, using a quasi-monochromatic source for irradiation of the sample and broadband detection of the reflected radiation. STARR is described extensively in [25], and a schematic is shown in Figure 2.

Briefly, a spherical mirror focuses radiant flux from the source through an order-sorting filter and a shutter onto the entrance slit of a single-grating monochromator. The beam emerging from the exit slit of the monochromator is incident on an iris to provide a circular incident beam, and is collimated by an off-axis parabolic mirror. The incident beam passes through a Glan-Taylor polarizer before passing through the sample goniometer. The beam is collected by the detector aperture, and is focused by a lens onto the detector, which produced a signal proportional to the radiant flux. (Refer to Table 1 for additional details.)

The spectral reflectance factor $R(\lambda,\sigma)$ is calculated based on the following equation:

$$R(\lambda,\sigma) = \frac{\pi \cdot {r_D}^2}{A_D \cdot \cos\theta_r} \cdot \frac{S_r'(\lambda,\sigma)}{S_i'(\lambda,\sigma)} \qquad (2)$$

where r_D is the distance between the sample and the aperture of the detector, A_D is the area of this aperture, and θ_r is the detection angle of the reflected radiation. $S_r'(\lambda)$ is the net signal due to the reflected radiation and $S_i'(\lambda)$ is the net signal due to the incident radiation, such that both signals are corrected for the dark current.

The comparison items were placed in the sample holder with the dorsal orientation mark upright. For each wavelength and polarization, the signals are collected in the following sequence: incident signal, dark signal in the incident position, reflected signal, dark signal in the reflected position, incident signal, and dark signal in the incident position. Dark signals are obtained by closing the shutter on the monochromator, and the net signals for the incident and reflected positions are obtained by subtracting the dark signals. The average net signal due to the incident radiation, acquired before and after each measurement of the reflected signal, is used to minimize the effects of source drift and fluctuations on the timescale of a single reflectance measurement. The reflectance factors acquired for each polarization, 0° and 90°, are averaged to yield the reflectance factor for unpolarized incident radiation.

2 NIST Goniospectrometer

The NIST Goniospectometer consists of a monochromatic illuminator, a white light illuminator, a 0:45 color wheel, a five-axis goniometer, and receivers [13,26–28]. A schematic of the instrument is shown in Figure 3. Briefly, the light passes through an order-sorting filter, a double-grating monochromator, a telecentric aperture, an optical chopper, an elliptical focusing mirror, a beam-splitting window, and a polarization scrambler. The radiant flux reflected from the beam-splitting window is measured with a monitor detector, which consists of a lens, a precision aperture, and a 10 mm by 10 mm silicon photodiode. A folding mirror is used to select between two measurement geometries: 0:45 color wheel and the five-axis goniometer. For all measurements, the comparison items were placed in the sample holder with the dorsal orientation mark upright.

Two measurement configurations can be implemented with the NIST Goniospectrometer. The first is the 0:45 color wheel, which was designed to make relative measurements. The illumination and viewing angles are fixed at 0° and 45°, respectively, while a sample wheel containing the comparison items and reference reflectance standards rotates through each sample position (up to 20). At each wavelength, reflected signals are measured for each position of the sample wheel containing an item.

To determine the 0:45 reflectance factor of the comparison items, the reflected signals are compared to reference standards, whose 0:45 reflectance factors have been determined using the NIST STARR facility. Thus, the reflectance factor $R(\lambda,\sigma)$, obtained using the 0:45 color wheel, at each wavelength λ and polarization σ is given by

$$R(\lambda,\sigma) = \frac{S(\lambda,\sigma)}{S_S(\lambda,\sigma)} R_S(\lambda,\sigma) \qquad (3)$$

where S and S_s are the measured signals from the item and standard, respectively, and R_s is the reflectance factor of the reference standard. These signals are collected in AC mode using a mechanical chopper and phase-sensitive detection.

The second measurement configuration implemented with the NIST Goniospectrometer is the five-axis goniometer, which allows bidirectional reflectance measurements over a wide range of illumination and viewing angles for in-plane and out-of-plane geometries. The sample can be moved about three different axes, allowing illumination and viewing for any direction within the hemisphere about the sample. The five-axis goniometer enables absolute reflectance measurements.

The spectral component of reflectance can be determined in two ways using the five-axis goniometer. In the first case, the incident beam is generated using the lamp and monochromator system described above and a single element silicon (Si) photodiode is installed on the receiver arm of the five-axis goniometer. This case mirrors the measurement method of NIST STARR with two important differences: limited spectral range (visible region only) and reduced stray light component for color samples with smaller uncertainties. It was validated through a comparison measurement with the NIST STARR facility. The two instruments agreed to within 0.5 % [12].

In the second case, a broadband source illuminates the sample and a fiber-coupled CCD array spectrometer is mounted on the receiver arm of the five-axis goniometer [28]. The array spectrometer is corrected for spectrally stray light and a neutral density (ND) filter is used for the measurement of the reference flux to increase the available dynamic range. This case was validated in a comparison with the 0:45 color wheel [29]. For measurements above 500 nm, the instruments agreed within 0.5 %.

For both cases employing the five-axis goniometer, the spectral reflectance factor $R(\lambda)$ at each wavelength is calculated using

$$R(\lambda) = \frac{\pi \cdot {r_D}^2}{A_D \cdot \cos\theta_r} \cdot \frac{S_r'(\lambda)}{S_i'(\lambda)} \qquad (4)$$

where, r_D is the distance between the sample and the aperture of the detector, A_D is the area of this aperture, and θ_r is the detection angle of the reflected radiation. $S_r'(\lambda)$ is the net signal due to the reflected radiation and $S_i'(\lambda)$ is the net signal due to the incident radiation.

3. Uncertainty analysis

A set of uncertainty components for the absolute bidirectional reflectance measurements is common among the different instruments described above. These include Type B components caused by the geometry of the instrument, such as angles of incidence and reflection, aperture distance and area, and location of the sample; wavelength discrimination; stray light; and linearity of the detector. The Type A component is due to random effects, such as detector noise. Depending on the instrument, the Type A component may either be calculated from the uncertainty in the signals or the standard deviation of repeat measurements.

Additionally, there are uncertainty components unique to each instrument. For the PTB Gonioreflectometer, these Type B components are lamp stability and the temperature dependence of the sphere aperture. For the NIST five-axis goniospectrometer with CCD detection system, there is a Type B component due to the transmittance of the ND filter, which is used with the CCD array spectrometer. Also, there is a Type B component for the NIST STARR and five-axis goniospectrometer (both detection methods) due to approximations made in the solid angle calculations.

The sources of uncertainty and their contributions, expressed in absolute terms, for the absolute bidirectional reflectance measurements are reported for each instrument and comparison item in Tables 2, 3, 5, and 6.

The set of uncertainty components for the relative bidirectional reflectance measurements is simplified in comparison. These sources and their contributions are reported in Table 4. The design of the instrument (fixed angles of incidence and reflection) and use of the substitution method eliminate the uncertainty contributions due to geometrical effects. Uncertainty due to detector linearity is evaluated together with uncertainty due to misalignment of the sample and/or reference standard and reported under the term offset. Additionally, there is an uncertainty component due to the reference standard [27].

Uncertainties are calculated in accordance with the procedures outlined in the Guide to the Expression of Uncertainty in Measurement (GUM) [30]. The final uncertainty, as stated in Tables 2 through 6, is the expanded measurement uncertainty, which is obtained by multiplying the combined measurement uncertainty from all uncertainty contributions by the coverage factor $k = 2$. Use of this coverage factor means that that 95% of intervals constructed in this manner will include the true value of the measurand.

4. Results and Discussion

The reflectance factors of each comparison item were determined according to the respective measurement equation of each instrument as detailed above. Example plots of these values are shown in Figure 4 for PTFE #1 and Ceramic #45. Visual inspection of the spectra in each figure indicates good agreement between the various instruments.

Agreement between a pair of instruments is described quantitatively by calculating the difference between the values of reflectance factors obtained by each instrument and comparing the difference to the combined expanded uncertainty ($k = 2$) of the two instruments. The resulting agreement between the national reference instruments of PTB and NIST for each comparison item is shown in Figure 5. Figures 6, 7, and 8 show the resulting agreement between the various measurement configurations of the NIST Goniospectrometer and NIST STARR for each comparison item. (Due to time restrictions, the

five-axis goniospectrometer with Si photodiode only measured Ceramic #46; the agreement with NIST STARR is limited to this comparison item only as shown in Figure 8.) Overall, the differences in reflectance values fall within the combined expanded uncertainty, indicating good agreement between each pair of instruments. This suggests that each instrument is supported by reasonable uncertainty budgets and substantiates the quality of measurements obtained by these instruments.

The results also highlight the need for improvement in some areas. Common to all plots is the increasingly negative difference for Ceramic #46 as the wavelength decreases from approximately 450 nm to 330 nm. This suggests that the values for reflectance factor obtained by STARR for this sample were too large in comparison to the values obtained by PTB and the NIST Goniospectrometer. Several possible reasons may explain the larger than expected values.

Differences in the bandwidth or bandpass of the instruments may account for the discrepancy in comparison results. NIST STARR has the largest bandwidth for its source, 14 nm. The bandwidth for PTB's detection system is 3 nm (for wavelengths less than 900 nm), and the bandwidth for the NIST Goniospectrometer is 5 nm. Thus, PTB and NIST goniospectrometers can more precisely measure the rapidly changing reflectance values of the ceramic samples below 450 nm compared to NIST STARR. However, the differences between NIST STARR and the other instruments are well within the expanded uncertainties for Ceramic #45, suggesting that the bandwidth of NIST STARR is not a significant influence.

Another possible reason may be the different stray light uncertainties of the instruments. NIST STARR uses a single monochromator with broadband detection, which results in a stray light uncertainty of 10^{-4}. The PTB gonioreflectometer also has a single monochromator, but it uses broadband illumination with monochromatic detection to reduce its stray light uncertainty to 10^{-5}. The NIST Goniospectrometer reduces its stray light uncertainty to 10^{-6} by using a double additive monochromator. (There is broadband detection for the configurations 0:45 color and five-axis goniometer with Si detector, and monochromatic detection for the configuration with the five-axis goniometer with CCD detection system.) If there were fluorescence from sample or other stray light, it would contribute most significantly to measurements obtained with NIST STARR. However, the results for Ceramic #45 do not show the same trend as Ceramic #46, suggesting that the trend is not due to fluorescence. Additionally, the lack of a systematic bias for all samples suggests that stray light is also not responsible.

Between 330 nm and 450 nm, the reflectance values for the ceramic samples are changing rapidly. A shift in the wavelength scale in this spectral region could significantly affect the values of reflectance factors. NIST has discovered in the time since the completion of this intercomparison that the mechanical movements involved in switching between the xenon arc and quartz-tungsten-halogen lamps were unstable and could result in a wavelength shift of several tenths of a nanometer. It is possible that a shift in the wavelength scale occurred temporarily affecting measurement of Ceramic #46 and resulting in larger than expected values. Procedures and checks are now in place to verify the wavelength scale and prevent such errors.

In addition to the trend seen for Ceramic #46, a larger-than-expected difference between the reflectance values obtained by NIST STARR and the 0:45 color configuration of the NIST Goniospectrometer is observed for PTFE #2. Because other samples have reasonable agreement and 0:45 color is directly referenced to NIST STARR, it is likely due to an alteration in the alignment of the sample pocket in the 0:45 color wheel.

5. Conclusion

We have presented the results of a bilateral comparison of bidirectional reflectance scales of NIST and PTB. The scales for reflectance factor in 0:45 geometry for PTB and NIST STARR were found to be in good agreement within the combined expanded uncertainty ($k = 2$) in the investigated spectral range 330 nm to 1150 nm. Further, the 0:45 reflectance factor scales of NIST STARR and the various measurement configurations of the NIST Goniospectrometer were found to be in good agreement. These results demonstrate the equivalence of the measurements produced by each of the instruments despite the varying designs and methods. They also provide critical evidence of the comparability of the NIST's and PTB's bidirectional reflectance scales in the absence of a key comparison.

In the near future, we plan to extend the number of compared geometrical configurations to include the industrial relevant geometries of 45:–30, 45:–20, 45:0, 45:30 and 45:65 as recommended in ASTM E2539-8 and realized in many commercial multi-angle spectrophotometers [18].

References

1. M. E. Nadal and E. A. Early, "Color measurements for pearlescent coatings," Color Res. Appl. 29, 38-42 (2004).
2. T. Atamas, K.-O. Hauer, and A. Höpe, "Appearance measurements of goniochromatic colours," in Predicting Perceptions: Proceedings of the 3rd International Conference on Appearance, S. Padilla, ed. (International Society for Presence Research, 2012), pp. 149-154.

3. A. Höpe, A. Koo, F. M. Verdú, F. B. Leloup, G. Obein, G. Wübbeler, J. Campos, P. Iacomussi, P. Jaanson, S. Källberg, and M. Šmíd, " 'Multidimensional reflectometry for industry' (xD-Reflect) an European research project," Proc. SPIE 9018, 901804 (2014).
4. P. Wißling, Metallic Effect Pigments (Vincentz Network GmbH & Co KG, 2006).
5. G. Pfaff, Special Effect Pigments (Vincentz Network GmbH & Co KG, 2008).
6. G. A. Klein, Industrial Color Physics (Springer Series in Optical Sciences, 2010).
7. A. Höpe, K.-O. Hauer, P. Bergner, T. Ziegler, "BRDF measurements at 254 nm for the LISA Pathfinder satellite mission," in Proceedings of NEWRAD, S. Park, P. Kärhä, E. Ikonen, ed. (NEWRAD, 2014), pp. 326-329 .
8. W. Gurlit, H. Bösch, H. Bovensmann, J. P. Burrows, A. Butz, C. Camy-Peyret, M. Dorf, K. Gerilowski, A. Lindner, S. Noël, U. Platt, F. Weidner, and K. Pfeilsticker, "The UV-A and visible solar irradiance spectrum: inter-comparison of absolutely calibrated, spectrally medium resolution solar irradiance spectra from balloon- and satellite-borne measurements," Atmos. Chem. Phys. 5, 1879–1890 (2005).
9. D. R. Taubert, J. Hollandt, P. Sperfeld, S. Pape, A. Höpe, K.-O. Hauer, P. Gege, T. Schwarzmaier, K. Lenhard, and A. Baumgartner, "Providing radiometric traceability for the Calibration Home Base of DLR by PTB," in AIP Conf. Proc. 1531, (AIP, 2013), pp. 376-379.
10. D. Hünerhoff, U. Grusemann, and A. Höpe, "New robot-based gonioreflectometer for measuring spectral diffuse reflection," Metrologia 43, S11–16 (2006).
11. A. Höpe, D. Hünerhoff, and K.-O. Hauer, "Robot-based gonioreflectometer," in Industrial Robotics: Programming, Simulation, and Applications, K-H Low, ed. (Mammendorf: Pro Literatur-Verlag, 2007), pp. 623-632.
12. G. Obein, R. Bousquet, and M. E. Nadal, "New NIST Reference Goniospectrometer," Proc. SPIE, 5880, 241-250 (2005).
13. M. E. Nadal, E. A. Early, W. Weber, and R. Bousquet, "NIST 0:45 Reflectometer," Color Res. Appl. 33, 94-99 (2008).
14. A. M. Rabal, A. Ferrero, J. Campos, J. L. Fontecha, A. Pons, A. M. Rubiño and A Corróns, "Automatic gonio-spectrophotometer for the absolute measurement of the spectral BRDF at in- and out-of-plane and retroreflection geometries", Metrologia 49, 213-223 (2012).
15. R. Baribeau, W. S. Neil, É. Côte, "Development of a robot-based gonioreflectometer for spectral BRDF measurement", J. Mod. Opt., 56, 1497-1503 (2009).
16. F. B. Leloup, S. Forment, P. Dutré, M. R. Pointer, Peter Hanselaer, "Design of an instrument for measuring the spectral bidirectional scatter distribution function", Appl. Opt. 47, 5454-5467 (2008).
17. DIN 6175-2:2001-03, Tolerances for automotive paints – Part 2: Goniochromatic paints, Beuth Verlag GmbH, Berlin (2001).
18. ASTM E2539-08, Standard Practice for Multiangle Color Measurement of Interference Pigments, ASTM International, West Conshohocken, PA (2008).
19. M. Nadal, K. L. Eckerle, E. A. Early, and Y. Ohno, "Final report on the key comparison CCPR-K5: Spectral diffuse reflectance," Metrologia 50, 02003 (2013).
20. Mutual recognition of national measurement standards and of calibration and measurement certificates issued by national metrology institutes (Comité International des Pois et Mesures, 14 October 1999). Technical Supplement (pp. 38-41) revised in October 2003.
21. F. E. Nicodemus, J. C. Richmond, J. J. Hsia, I. W. Ginsberg, and T. Limperis, "Geometrical considerations and nomenclature for reflectance," NBS Monograph 160 (1977).
22. CIE 15:2004, Colorimetry, International Commission on Illumination (2004).
23. S. Holopainen, F. Manoocheri, E. Ikonen, K.-O. Hauer, and A. Höpe, "Comparison measurements of 0:45 radiance factor and goniometrically determined diffuse reflectance," Appl. Opt. 48, 2946–2956 (2009).
24. K.-O. Hauer and A. Höpe, "High-grade uniform light source for radiometric and photometric applications," MAPAN J. Metrol. Soc. India 24, 175-182 (2009).
25. P. Y. Barnes, E. A. Early, and A. C. Parr, "NIST Measurement Services: Spectral Reflectance," NIST Special Publication 250-48 (1995).
26. M. E. Nadal, E. A. Early, and R. Bousquet, "NIST Measurement Services: 0:45 Surface Color," NIST Special Publication 250-71 (2008).
27. E. A. Early and M. E. Nadal, "Uncertainty Analysis for the NIST 0:45 Reflectometer," Color Res. Appl. 33, 100-107 (2008).
28. M. E. Nadal and G. Obein, "NIST Goniospectrometer for Surface Color Measurements," in CIE Expert Symposium on Advances in Photometry and Colorimetry (CIE, 2008), pp. 134-138.
29. V. B. Podobedov, C. C. Miller, and M. E. Nadal, "Performance of the NIST Five-Axis Goniometer with Broad-Band Source and Multichannel CCD based Spectrometer," Rev. Sci. Instrum. 83, 093108 (2012).
30. ISO/IEC Guide 98-3:2008: Uncertainty of measurement – Part 3: Guide to the expression of uncertainty in measurement

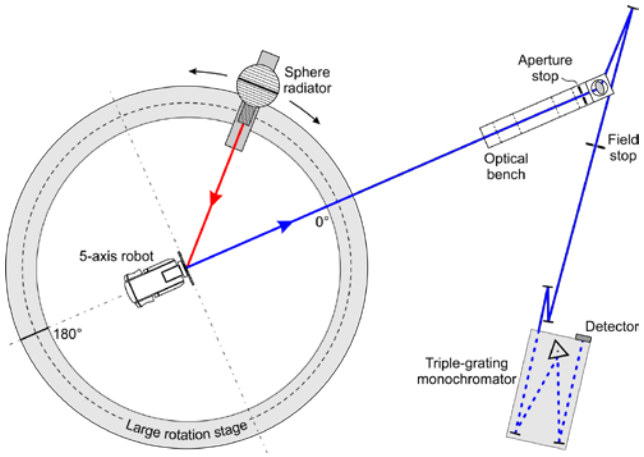

Fig. 1. Schematic of the PTB robot-based gonioreflectometer with the main components of the set-up indicated.

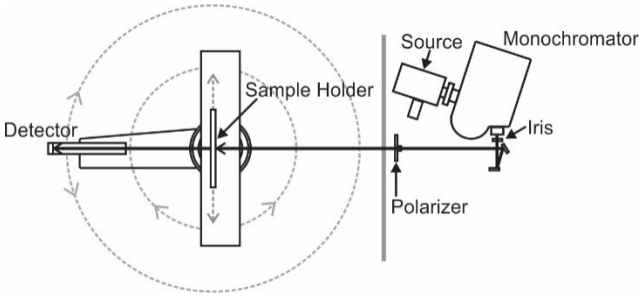

Fig. 2. Schematic of STARR's bidirectional measurement system with major components labeled.

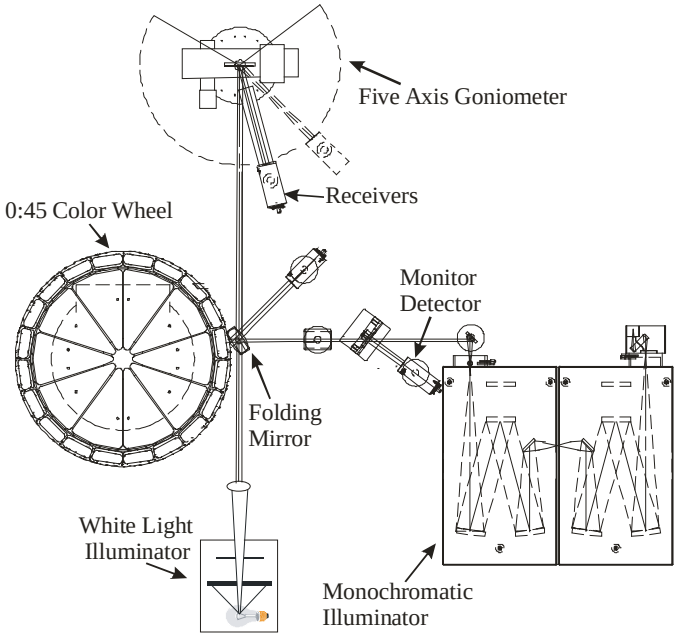

Fig. 3. Schematic of the NIST goniospectrometer with the major components labeled.

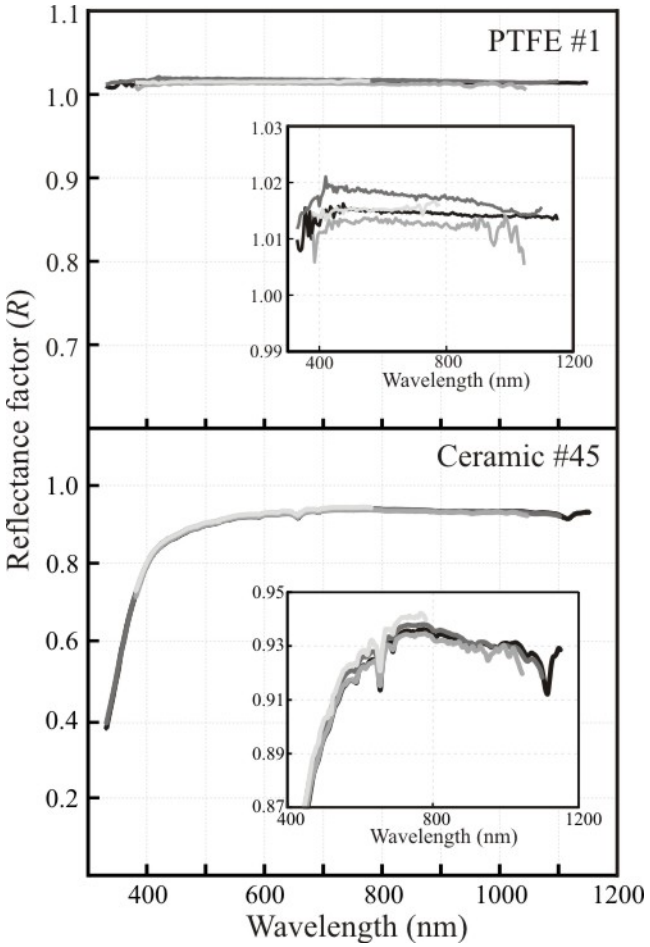

Fig. 4. 0:45 spectral reflectance factor R as measured by PTB (black), STARR (dark grey), the 0:45 color wheel (light grey), and the five-axis goniometer with CCD detection system (medium grey). The top panel shows the results for PTFE #1 and the bottom panel shows the results for Ceramic #45. Magnified views of the spectra are provided in the insets.

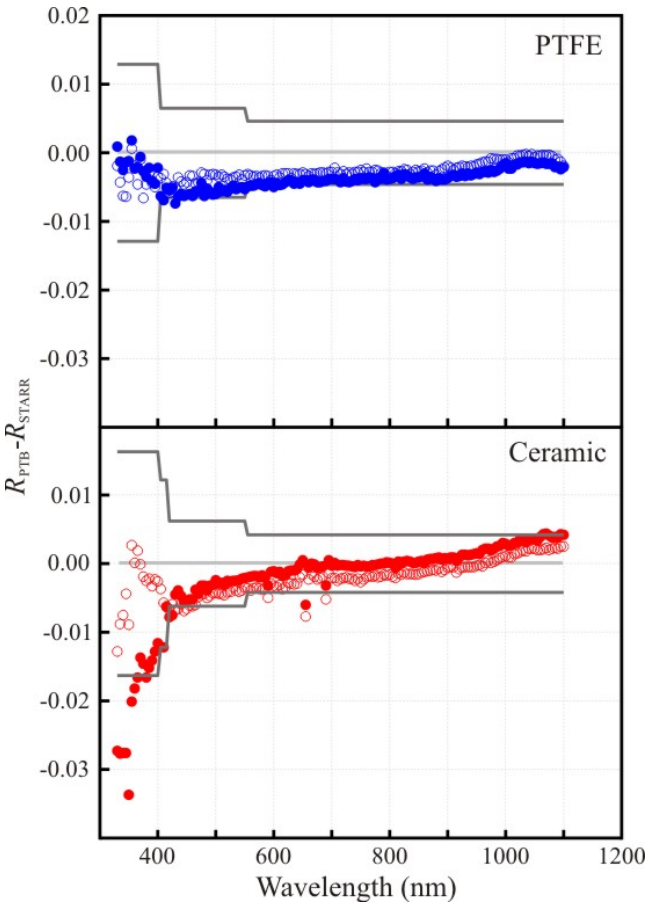

Fig. 5. Difference between spectral reflectance factors measured by PTB and by STARR, R_{PTB}-R_{STARR}. The top panel shows the results for PTFE #1 (open circles) and PTFE #2 (filled circles). The bottom panel shows the results for Ceramic #45 (open circles) and Ceramic #46 (filled circles). The upper and lower bounds depicting the combined expanded uncertainty ($k = 2$) of the difference are indicated by the dark grey lines.

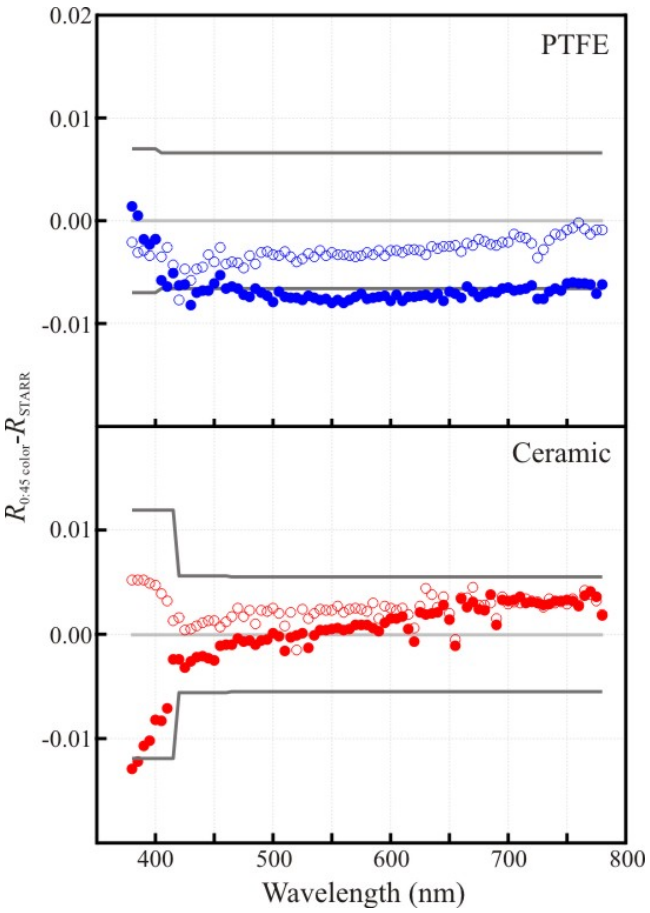

Fig. 6. Difference between spectral reflectance factors measured by 0:45 color wheel and by STARR, $R_{0:45\ color}$–R_{STARR}. The top panel shows the results for PTFE #1 (open circles) and PTFE #2 (filled circles). The bottom panel shows the results for Ceramic #45 (open circles) and Ceramic #46 (filled circles). The upper and lower bounds depicting the combined expanded uncertainty ($k = 2$) of the difference are indicated by the dark grey lines.

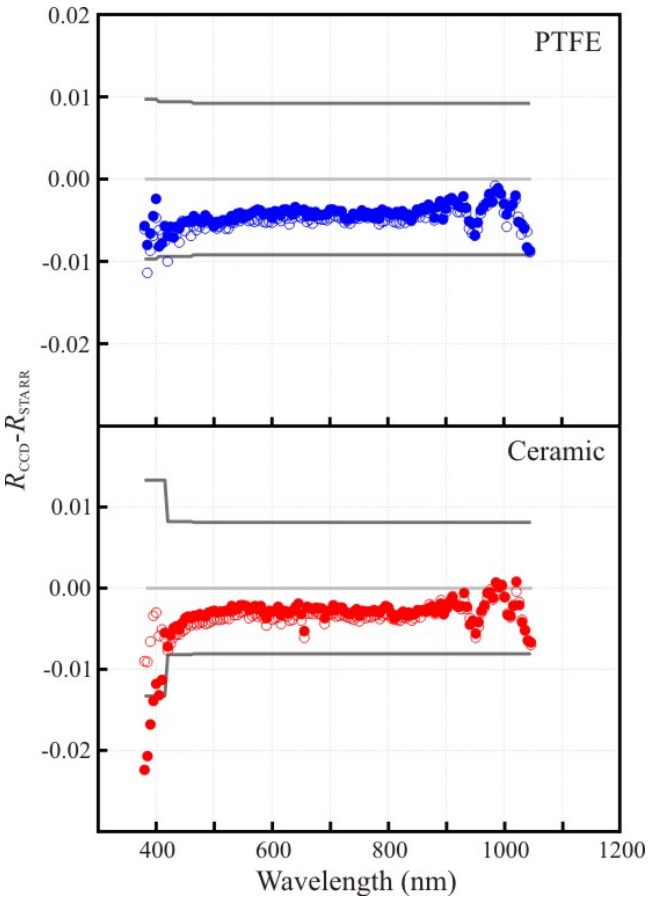

Fig. 7. Difference between spectral reflectance factors measured by five-axis goniometer with CCD detection system and by STARR, R_{CCD}–R_{STARR}. The top panel shows the results for PTFE #1 (open circles) and PTFE #2 (filled circles). The bottom panel shows the results for Ceramic #45 (open circles) and Ceramic #46 (filled circles). The upper and lower bounds depicting the combined expanded uncertainty ($k = 2$) of the difference are indicated by the dark grey lines.

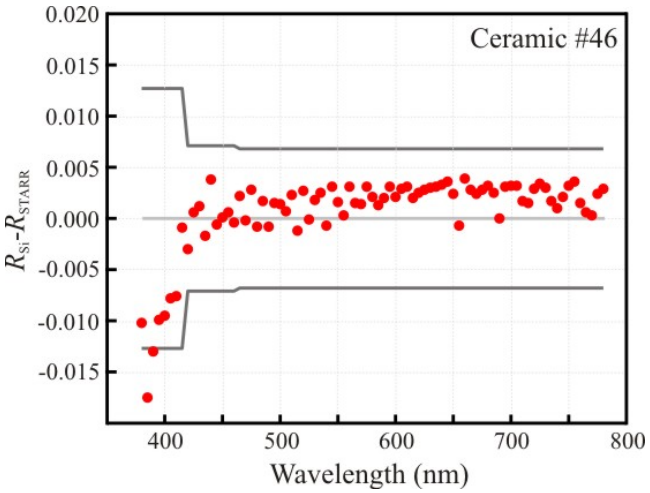

Fig. 8. Difference between spectral reflectance factors measured by five-axis goniometer with Si photodiode and by STARR, R_{Si}–R_{STARR}, for Ceramic #46. The upper and lower bounds depicting the combined expanded uncertainty ($k = 2$) of the difference are indicated by the dark grey lines.

Table 1. Parameters of each instrument participating in this comparison.

			NIST Goniospectrometer		
Parameters	PTB Gonioreflectometer	NIST STARR	0:45 color wheel	5-axis gonio. with Si photodiode	5-axis gonio. with CCD array
Measurement Method	Absolute	Absolute	Relative	Absolute	Absolute
Spectral Determination Method	Broadband source; monochromatic detection	Monochromatic source; broadband detection	Monochromatic source; broadband detection	Monochromatic source; broadband detection	Broadband source; monochromatic detection
Source	QTH lamp	Xenon arc lamp ($\lambda \leq 400$ nm) QTH lamp ($\lambda > 400$ nm)	Xenon arc lamp ($\lambda \leq 460$ nm) QTH lamp ($\lambda > 460$ nm)	Xenon arc lamp ($\lambda \leq 460$ nm) QTH lamp ($\lambda > 460$ nm)	Xenon arc lamp ($\lambda \leq 460$ nm) QTH lamp ($\lambda > 460$ nm)
Detector	Solar blind CPM (250 nm to 350 nm) Yellow enhanced CPM (300 nm to 450 nm) Si photodiode (400 nm to 1150 nm)	UV-enhanced Si photodiode	Si photodiode	Si photodiode	CCD array spectrometer
Bandwidth/pass	3 nm ($\lambda < 900$ nm) 6 nm ($\lambda \geq 900$ nm)	14 nm	5 nm	5 nm	3.7 nm
Aperture distance	781.8 mm	669.9 mm	292 mm	1250.0 mm	1250.0 mm
Aperture area	1256.6 mm^2	796.7 mm^2	9.90 mm^2	2744.9 mm^2	2744.9 mm^2
Beam size	20 mm diameter (at detection)	17 mm diameter (at sample)	10 mm × 12 mm (at sample)	10 mm × 12 mm (at sample)	10 mm × 12 mm (at sample)
Wavelength range	250 nm to 1700 nm	250 nm to 1100 nm	380 nm to 780 nm	380 nm to 780 nm	300 nm to 1050 nm

Table 2. Uncertainty contributions and expanded uncertainty ($k = 2$) of the 0:45 spectral reflectance factor $R(\lambda)$ of the matte ceramic and sintered PTFE reflectance standards, as determined by PTB.

		Absolute Uncertainty Contribution	
Source of Uncertainty	Standard Uncertainty	Ceramic Reflectance Standard, Serial Nos. 45 and 46	PTFE Reflectance Standard, Serial Nos. 1 and 2
Aperture Distance	0.07 mm	0.0001	0.0001
Aperture Area	0.07 mm^2	0.00007	0.00007
Location of Sample	0.3 mm	0.0005	0.0005
Angle of Incidence	0.2°	0.0001	0.0001
Angle of Detection	0.2°	0.0002	0.0002
Wavelength	0.2 nm	0.0012 (330 nm ≤ λ ≤ 400 nm)	2·10-5 (330 nm ≤ λ ≤ 400 nm)
		0.0001 (400 nm ≤ λ ≤ 550 nm)	7·10-6 (400 nm ≤ λ ≤ 550 nm)
		3.3·10-6 (550 nm ≤ λ ≤ 1150 nm)	2·10-6 (550 nm ≤ λ ≤ 1150nm)
Stray Light	$5 \cdot 10^{-5}$	$5 \cdot 10^{-5}$	$5 \cdot 10^{-5}$
Detector Linearity	0.0001	0.0002	0.0002
Signals/Repeatability		0.0058 (330 nm ≤ λ ≤ 400 nm)	0.0058 (330 nm ≤ λ ≤ 400 nm)
		0.0024 (400 nm ≤ λ ≤ 550 nm)	0.0024 (400 nm ≤ λ ≤ 550 nm)
		0.0009 (550 nm ≤ λ ≤ 1150 nm)	0.0009 (550 nm ≤ λ ≤ 1150 nm)
Lamp stability	$2 \cdot 10^{-5}$	$2 \cdot 10^{-5}$	$2 \cdot 10^{-5}$
Temp. dep. Aperture	5 K	0.0001	0.0001
		Expanded Uncertainty ($k = 2$)	
		0.012 (330 nm ≤ λ ≤ 400 nm)	0.012 (330 nm ≤ λ ≤ 400 nm)
		0.005 (400 nm ≤ λ ≤ 550 nm)	0.005 (400 nm ≤ λ ≤ 550 nm)
		0.002 (550 nm ≤ λ ≤ 1150 nm)	0.002 (550 nm ≤ λ ≤ 1150 nm)

Table 3. Uncertainty contributions and expanded uncertainty ($k = 2$) of the 0:45 spectral reflectance factor $R(\lambda)$ of the matte ceramic and sintered PTFE reflectance standards, as determined by STARR.

		Absolute Uncertainty Contribution	
Source of Uncertainty	Standard Uncertainty	Ceramic Reflectance Standard, Serial Nos. 45 and 46	PTFE Reflectance Standard, Serial Nos. 1 and 2
Aperture Distance	0.5 mm	0.0008	0.0009
Aperture Area	1.0 mm^2	0.0005	0.0006
Location of Sample	0.3 mm	0.0005	0.0006
Angle of Incidence	0.06°	0.0003	0.0004
Angle of Detection	0.06°	0.0009	0.0011
Wavelength	1 nm	0.0091 (330 nm ≤ λ ≤ 445 nm)	0.0004 (330 nm ≤ λ ≤ 400 nm)
		0.0002 (450 nm ≤ λ ≤ 1100 nm)	0.0001 (405 nm ≤ λ ≤ 1100 nm)
Stray Light	10^{-4}	< 0.0001	< 0.0001
Detector Linearity	0.05 %	0.0009	0.0010
Signals/Repeatability		0.0051 (330 nm ≤ λ ≤ 415 nm)	0.0012 (330 nm ≤ λ ≤ 400 nm)
		0.0001 (420 nm ≤ λ ≤ 1100 nm)	0.0002 (405 nm ≤ λ ≤ 1100 nm)
Solid Angle Calc.	0.05 %	0.0004	0.0005
		Expanded Uncertainty ($k = 2$)	
		0.021 (330 nm ≤ λ ≤ 415 nm)	0.0048 (330 nm ≤ λ ≤ 400 nm)
		0.019 (420 nm ≤ λ ≤ 445 nm)	0.0041 (405 nm ≤ λ ≤ 1100 nm)
		0.0039 (450 nm ≤ λ ≤ 1100 nm)	

Table 4. Uncertainty contributions and expanded uncertainty ($k = 2$) of the 0:45 spectral reflectance factor $R(\lambda)$ of the matte ceramic and sintered PTFE reflectance standards, as determined by 0:45 color wheel.

		Absolute Uncertainty Contribution	
Source of Uncertainty	Standard Uncertainty	Ceramic Reflectance Standard, Serial Nos. 45 and 46	PTFE Reflectance Standard, Serial Nos. 1 and 2
Reference standard	0.002	0.0020	0.0020
Offset/(Misalignment and Linearity)	0.15 %	0.0012	0.0016
Wavelength	0.1 nm	0.0007 (380 nm ≤ λ ≤ 460 nm) < 0.0001 (465 nm ≤ λ ≤ 780 nm)	0.0003 (380 nm ≤ λ ≤ 460 nm) < 0.0001 (465 nm ≤ λ ≤ 780 nm)
Stray Light	10^{-6}	< 0.0001	< 0.0001
Signals/Repeatability		0.0005 (380 nm ≤ λ ≤ 460 nm) 0.00010 (465 nm ≤ λ ≤ 780 nm)	0.0004 (380 nm ≤ λ ≤ 460 nm) 0.0001 (465 nm ≤ λ ≤ 780 nm)
		Expanded Uncertainty (k = 2)	
		0.0050 (380 nm ≤ λ ≤ 460 nm) 0.0047 (465 nm ≤ λ ≤ 780 nm)	0.0052 (380 nm ≤ λ ≤ 460 nm) 0.0051 (465 nm ≤ λ ≤ 780 nm)

Table 5. Uncertainty contributions and expanded uncertainty ($k = 2$) of the 0:45 spectral reflectance factor $R(\lambda)$ of Ceramic #46, as determined by the five-axis goniometer with Si photodiode.

		Absolute Uncertainty Contribution
Source of Uncertainty	Standard Uncertainty	Ceramic Reflectance Standard, Serial No. 46
Aperture Distance	0.1 mm	0.0001
Aperture Area	1.0 mm^2	0.0002
Offset/(Misalignment)	0.15%	0.0014
Wavelength	0.1 nm	0.0007 (380 nm ≤ λ ≤ 460 nm) < 0.0001 (465 nm ≤ λ ≤ 1045 nm)
Stray Light	10^{-6}	< 0.0001
Detector Linearity	0.001	0.0020
Signals/Repeatability		0.0015 (380 nm ≤ λ ≤ 460 nm) 0.0005 (465 nm ≤ λ ≤ 1045 nm)
Solid Angle Calc.	0.06 %	0.0006
		Expanded Uncertainty (k = 2)
		0.0060 (380 nm ≤ λ ≤ 460 nm) 0.0051 (465 nm ≤ λ ≤ 780 nm)

Table 6. Uncertainty contributions and expanded uncertainty ($k = 2$) of the 0:45 spectral reflectance factor $R(\lambda)$ of the matte ceramic and sintered PTFE reflectance standards, as determined by the five-axis goniometer with CCD detection system.

		Absolute Uncertainty Contribution	
Source of Uncertainty	Standard Uncertainty	Ceramic Reflectance Standard, Serial Nos. 45 and 46	PTFE Reflectance Standard, Serial Nos. 1 and 2
Aperture Distance	0.1 mm	0.0001	0.0001
Aperture Area	1.0 mm^2	0.0002	0.0002
Offset/(Misalignment)	0.15%	0.0014	0.0014
Wavelength	0.1 nm	0.0003 (380 nm ≤ λ ≤ 460 nm)	0.0001 (380 nm ≤ λ ≤ 460 nm)
		< 0.0001 (465 nm ≤ λ ≤ 1045 nm)	< 0.0001 (465 nm ≤ λ ≤ 1045 nm)
Stray Light	10^{-6}	0.0003	0.0002
Detector Linearity	0.002	0.0030	0.0030
Signals/Repeatability		0.0009 (380 nm ≤ λ ≤ 460 nm)	0.0006 (380 nm ≤ λ ≤ 460 nm)
		0.0003 (465 nm ≤ λ ≤ 1045 nm)	0.0003 (465 nm ≤ λ ≤ 1045 nm)
ND filter transmittance		0.0020	0.0020
Solid Angle Calc.	0.06 %	0.0005	0.0006
		Expanded Uncertainty (k = 2)	
		0.0081 (380 nm ≤ λ ≤ 460 nm)	0.0079 (380 nm ≤ λ ≤ 460 nm)
		0.0079 (465 nm ≤ λ ≤ 780 nm)	0.0079 (465 nm ≤ λ ≤ 780 nm)